

# Investigating Discontinuous X-ray Irradiation as a Damage Mitigation Strategy for $[M(COD)Cl]_2$ Catalysts

## Supplementary Information

Nathalie K. Fernando,<sup>\*a</sup> Claire A. Murray,<sup>b</sup> Amber L. Thompson,<sup>c</sup> Katherine Milton,<sup>a</sup> Andrew B. Cairns,<sup>d</sup> and Anna Regoutz<sup>a,e</sup>

<sup>a</sup> Department of Chemistry, University College London, 20 Gordon Street, London, WC1H 0AJ, UK.

<sup>b</sup> Diamond Light Source Ltd, Diamond House, Harwell Science and Innovation Campus, Didcot, Oxfordshire, OX11 0DE, UK.

<sup>c</sup> Chemical Crystallography, Chemistry Research Laboratory, University of Oxford, South Parks Road, Oxford OX1 3QR, UK.

<sup>d</sup> Department of Materials, Imperial College London, Royal School of Mines, Exhibition Road, SW7 2AZ, UK.

<sup>e</sup> Present address: Department of Chemistry, Inorganic Chemistry Laboratory, South Parks Road, OX1 3QR, UK.

**Table S1:** The parameters and corresponding values included in the RADDOSE-3D input file for  $[Ir(COD)Cl]_2$  and  $[Rh(COD)Cl]_2$  used to estimate the doses in the powder XRD experiments at beamline I11 at Diamond Light Source, Didcot, UK. The same values were used in the studies presented in Fernando *et al.* 2021. [1]

RADDOSE parameter	Beamline I11, DLS (PXRD)	K-Alpha+ (XPS)
Crystal type	cylinder	cuboid
Crystal Dimension / $\mu m$	$300 \times 40000$	$60 \times 60 \times 60$
PixelsPerMicron	0.06	0.6
Container material type	mixture	N/A
Material mixture	pyrex	N/A
Container thickness / $\mu m$	10	N/A
Container density / g $cm^{-3}$	2.23	N/A
Beam type	Gaussian	Gaussian
Photon flux / photons/s	$1.5 \times 10^{14}$	$3.8 \times 10^{10}$
FWHM / $\mu m$	$2000 \times 600$	$326 \times 579$
Energy / keV	15	1.487
Collimation type	rectangular	circular
Collimation dimensions / $\mu m^2$	$2500 \times 800$	$300 \times 300$

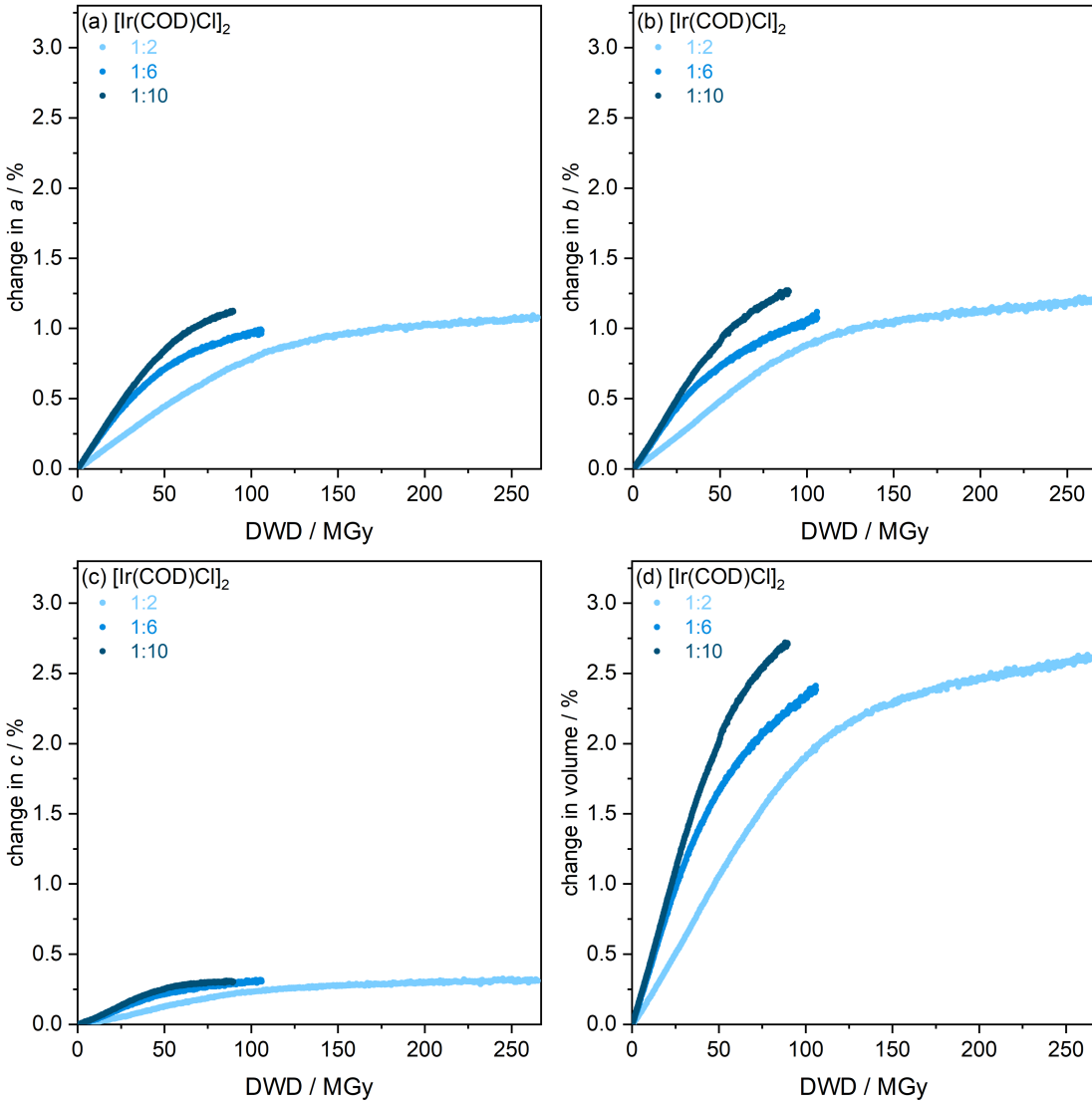


**Figure S1:** Percentage changes to lattice parameters and unit cell volume, with X-ray dose, for  $[\text{Ir}(\text{COD})\text{Cl}]_2$ , extracted from Le Bail refinements, for three X-ray irradiation to dark ratios for unit cell axes (a) *a*, (b) *b*, (c) *c* and (d) unit cell volume. From error propagation calculations, the approximate errors in (a)-(c) are  $\pm 0.007\%$ ,  $\pm 0.03\%$  and  $\pm 0.007\%$  for the 1:2, 1:6 and 1:10 datasets, respectively. Similarly, the errors for the change in volume, (d), are  $\pm 0.01\%$ ,  $\pm 0.06\%$  and  $\pm 0.02\%$ .

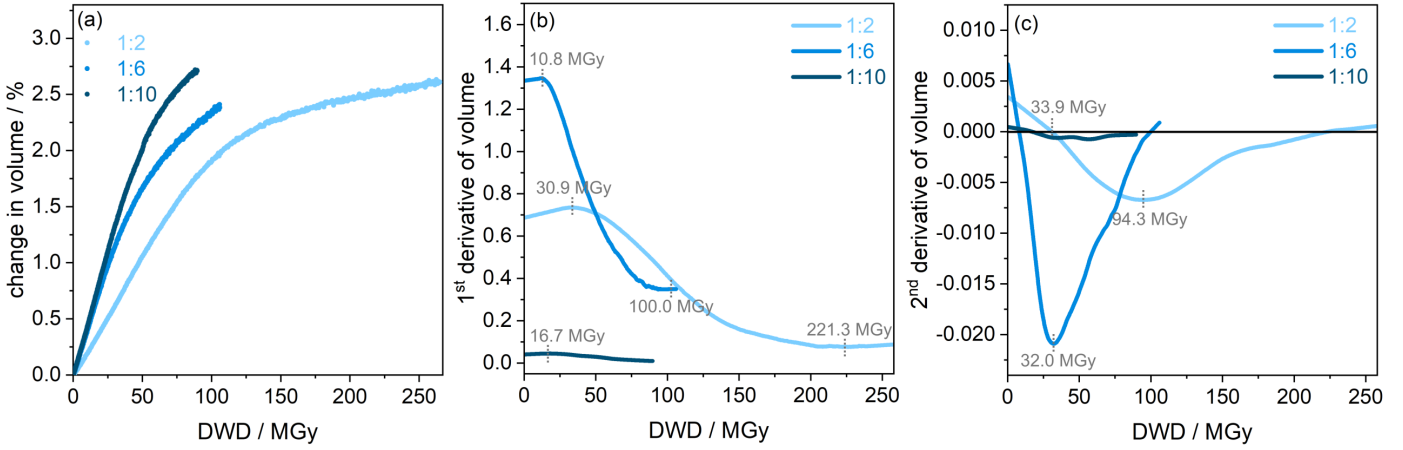


**Figure S2:** The changes in the curvature of the  $[\text{Ir}(\text{COD})\text{Cl}]_2$  unit cell volume for the 1:2, 1:6 and 1:10 X-ray irradiation/gap regimes as a function of X-ray dose to determine the onset of volume expansion saturation. (a) The percentage change in unit cell volume, (b) the first derivative curve of the volume with maximum and minimum points labelled, and (c) the second derivative of unit cell volume with points of inflection labelled.

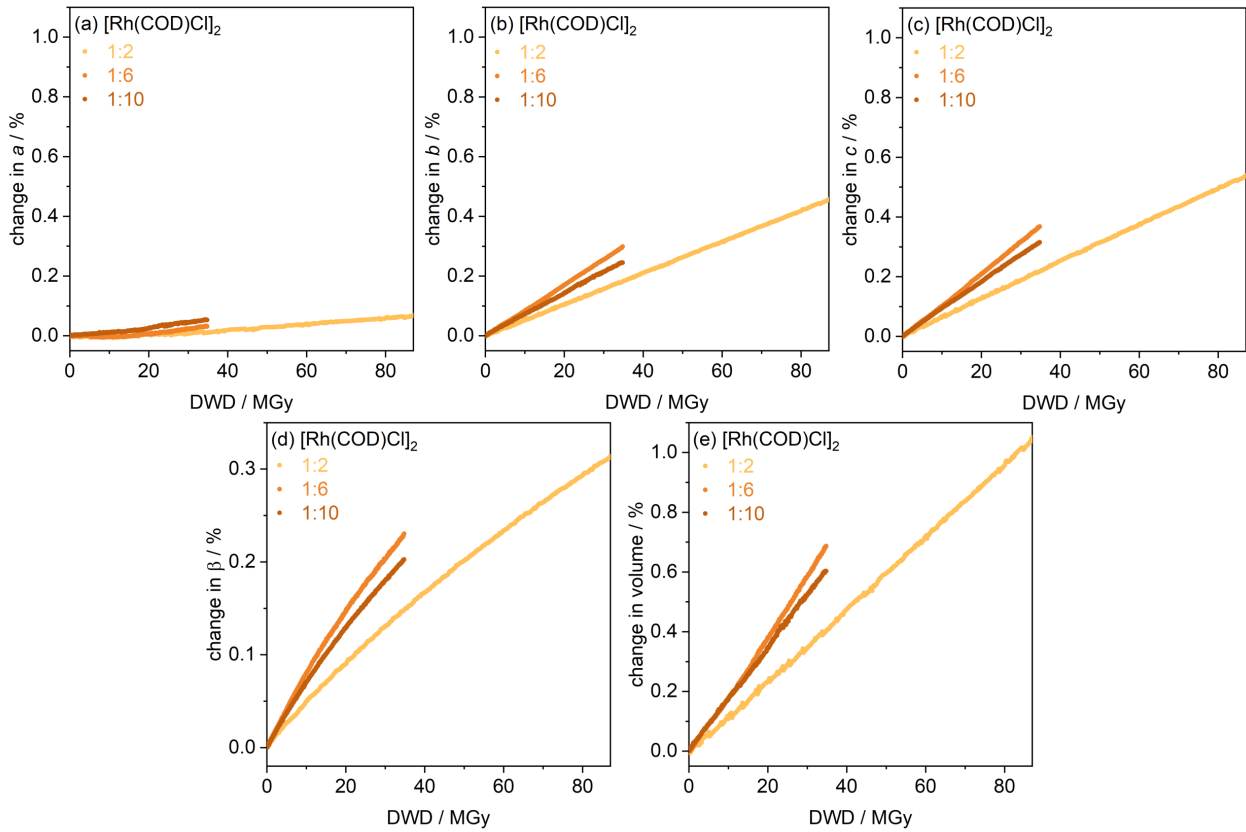


**Figure S3:** Percentage changes to lattice parameters for  $[\text{Rh}(\text{COD})\text{Cl}]_2$ , extracted from Le Bail refinements of the PXRD data as a function of X-ray dose and X-ray irradiation to dark ratios for unit cell axes (a)  $a$ , (b)  $b$ , (c)  $c$ , (d)  $\beta$  angle and (e) unit cell volume. From error propagation calculations of the last data point, the approximate errors in (a)-(c) are  $\pm 0.004\%$ ,  $\pm 0.001\%$  and  $\pm 0.002\%$  for the 1:2, 1:6 and 1:10 datasets, respectively. Similarly, the errors for the change in  $\beta$  (d), are  $\pm 0.001\%$  (for all 3 ratios) and for the change in volume, (e), these are  $\pm 0.01\%$ ,  $\pm 0.003\%$  and  $\pm 0.003\%$ .

**Table S2:** The interatomic distances and bond angles of  $[\text{Ir}(\text{COD})\text{Cl}]_2$  at the start of the XRD experiment and at a dose of 89 MGy, for the 1:2, 1:6 and 1:10 light:dark X-ray radiation regimes.

	Bond	1:2		1:6		1:10	
		start	end	start	end	start	end
Length(Å)	Ir1–Ir2	2.927(6)	2.91(1)	2.892(8)	2.86(2)	2.900(4)	2.84(2)
	Cl1–Cl2	2.89(3)	2.94(5)	2.98(4)	3.2(1)	2.99(2)	3.1(1)
	Ir1–Cl1	2.28(2)	2.29(3)	2.31(3)	2.26(7)	2.32(2)	2.29(7)
	Ir1–Cl2	2.25(2)	2.26(3)	2.29(3)	2.26(8)	2.32(2)	2.31(8)
	Ir2–Cl1	2.33(3)	2.33(4)	2.32(4)	2.29(9)	2.32(2)	2.31(9)
	Ir2–Cl2	2.29(2)	2.26(4)	2.31(3)	2.28(7)	2.31(2)	2.27(7)
Angle (°)	Cl1–Ir1–Cl2	79.2(9)	81(1)	81(1)	90(3)	80.20(7)	87(3)
	Cl1–Ir2–Cl2	77.8(9)	80(1)	80(1)	89(3)	80.20(7)	87(3)
	Ir1–Cl1–Ir2	79.0(8)	78(1)	77(1)	78(3)	77.30(6)	77(3)
	Ir1–Cl2–Ir2	79.9(8)	80(1)	77.8(9)	78(2)	77.50(6)	77(2)

**Table S3:** The interatomic distances and bond angles of  $[\text{Rh}(\text{COD})\text{Cl}]_2$  at the start of the XRD experiment and at a dose of 34.8 MGy, for the 1:2, 1:6 and 1:10 light:dark X-ray radiation regimes.

	Bond	1:2		1:6		1:10	
		start	end	start	end	start	end
Length (Å)	Rh1–Rh2	3.525(3)	3.543(3)	3.525(3)	3.540(3)	3.530(2)	3.539(3)
	Cl1–Cl2	3.167(8)	3.166(8)	3.295(8)	3.271(8)	3.285(7)	3.267(8)
	Rh1–Cl1	2.398(6)	2.414(6)	2.431(6)	2.449(6)	2.42(5)	2.422(6)
	Rh1–Cl2	2.374(6)	2.387(6)	2.424(6)	2.424(6)	2.450(6)	2.439(6)
	Rh2–Cl1	2.380(6)	2.364(6)	2.434(6)	2.403(6)	2.413(5)	2.364(6)
	Rh2–Cl2	2.345(6)	2.355(6)	2.376(6)	2.378(6)	2.380(5)	2.421(6)
Angle (°)	Cl1–Rh1–Cl2	83.1(2)	82.5(2)	85.5(2)	84.3(2)	84.9(2)	84.4(2)
	Cl1–Rh2–Cl2	84.2(2)	84.3(2)	86.5(2)	86.3(2)	86.5(2)	86.1(2)
	Rh1–Cl1–Rh2	95.1(2)	95.7(2)	92.8(2)	93.7(2)	93.8(2)	93.9(2)
	Rh1–Cl2–Rh2	96.7(2)	96.7(2)	94.5(2)	95.0(2)	93.9(2)	94.9(2)

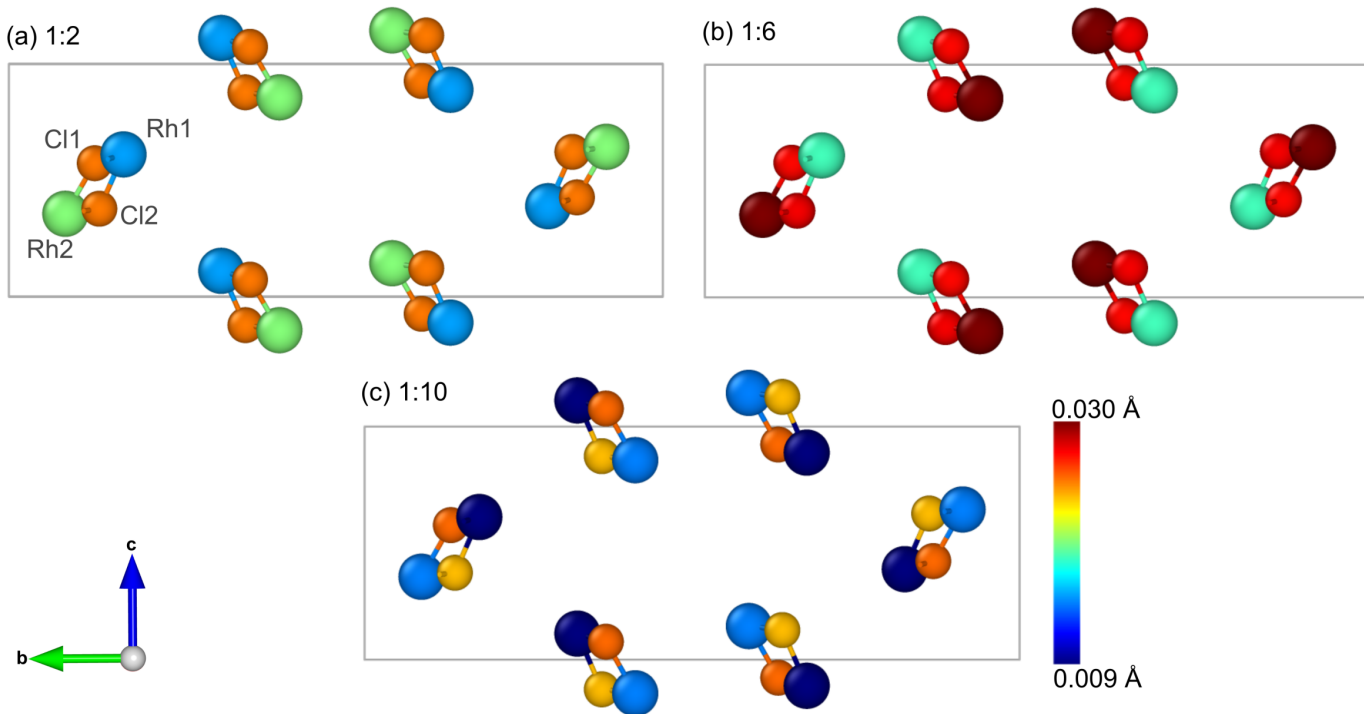


**Figure S4:** The magnitude of atomic displacements, in  $\text{\AA}$ , of the central M–Cl core of the  $[\text{Rh}(\text{COD})\text{Cl}]_2$  unit cell after an absorbed dose of 35 MGy, relative to the minimum dose structure for the three regimes of X-ray irradiation to X-ray-free ratios of (a) 1:2, (b) 1:6 and (c) 1:10. Figure produced using the Ovito software package. [2]

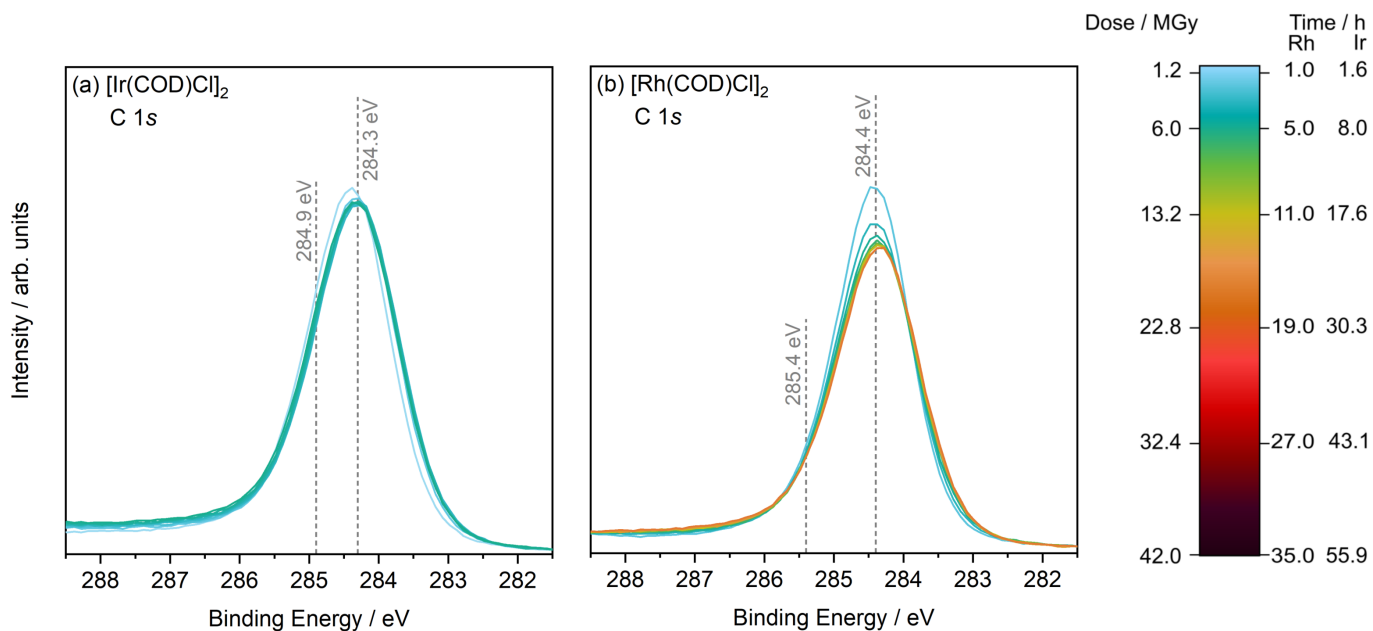


**Figure S5:** The iterative X-ray photoelectron C 1s spectra of (a)  $[\text{Ir}(\text{COD})\text{Cl}]_2$  and (b)  $[\text{Rh}(\text{COD})\text{Cl}]_2$  collected up to a maximum absorbed dose of 11 MGy and 19 MGy, respectively, when X-ray free gaps are incorporated into the experiment.

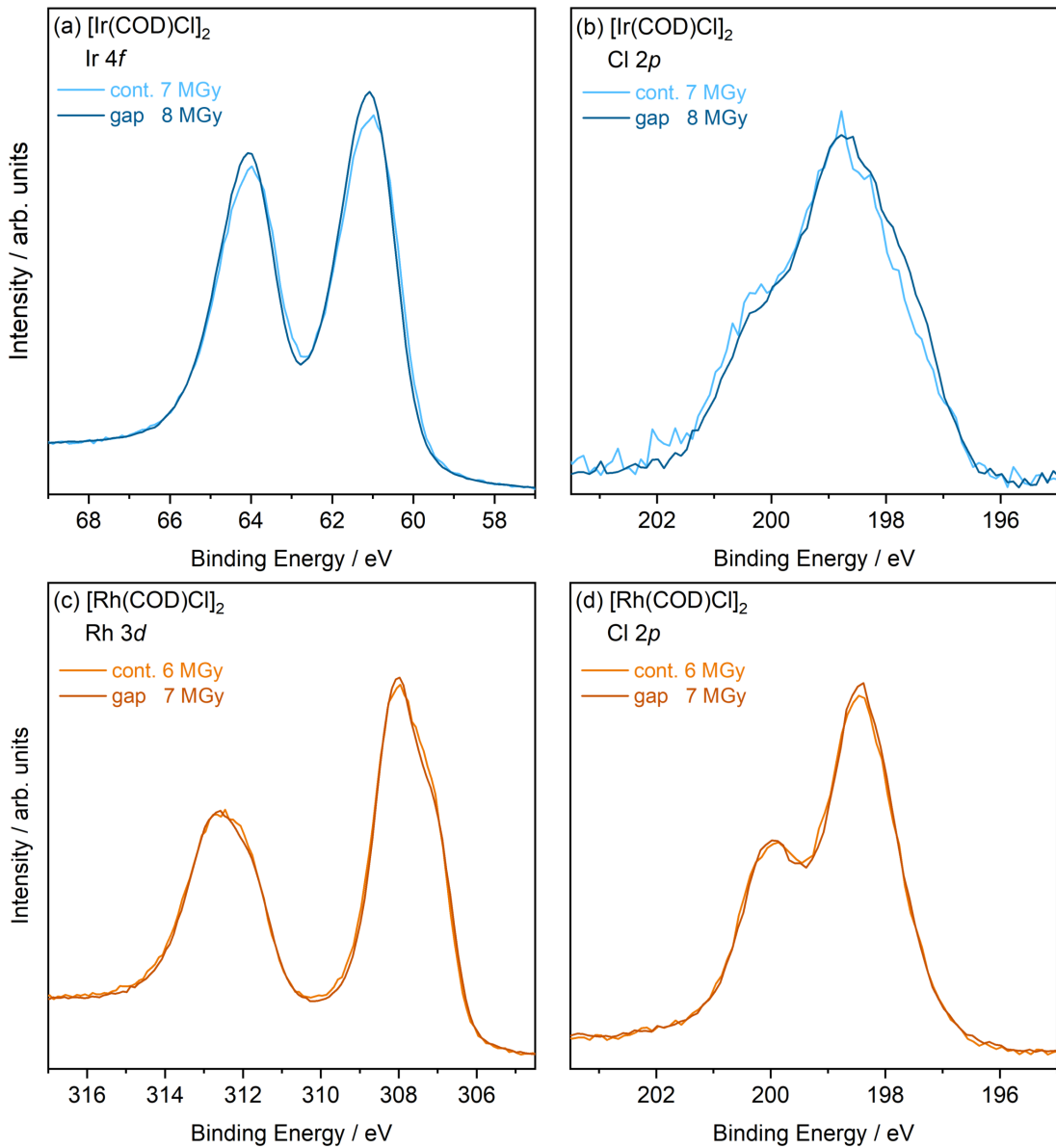


**Figure S6:** Comparison of the core level X-ray photoelectron spectra of the  $[M(\text{COD})\text{Cl}]_2$  catalysts measured under continuous irradiation and with X-ray-free gaps at  $\sim$ equal dose ( $\pm 1$  MGy), including (a) Ir 4f and (b) Cl 2p spectra of  $[\text{Ir}(\text{COD})\text{Cl}]_2$  and (c) Rh 3d and Cl 2p for  $[\text{Rh}(\text{COD})\text{Cl}]_2$ . The spectra are normalised to the area of the metal.

## References

- [1] N. K. Fernando, A. B. Cairns, C. A. Murray, A. L. Thompson, J. L. Dickerson, E. F. Garman, N. Ahmed, L. E. Ratcliff, and A. Regoutz. Structural and Electronic Effects of X-ray Irradiation on Prototypical  $[M(COD)Cl]_2$  Catalysts. *The Journal of Physical Chemistry A*, 125(34):7473–7488, 9 2021.
- [2] A. Stukowski. Visualization and analysis of atomistic simulation data with OVITO—the Open Visualization Tool. *Modelling and Simulation in Materials Science and Engineering*, 18(1):015012, 1 2010.